FERMILAB-PUB-23-499-V

Protecting backaction-evading measurements from parametric instability

E. P. Ruddy,[1, 2, *] Y. Jiang,[1, 2, *] N. E. Frattini,[1, 2] K. O. Quinlan,[1, 2] and K. W. Lehnert[1, 2]

[1] *JILA, National Institute of Standards and Technology and the University of Colorado, Boulder, Colorado 80309, USA*
[2] *Department of Physics, University of Colorado, Boulder, Colorado 80309, USA*

(Dated: August 22, 2023)

Noiseless measurement of a single quadrature in systems of parametrically coupled oscillators is theoretically possible by pumping at the sum and difference frequencies of the two oscillators, realizing a backaction-evading (BAE) scheme. Although this would hold true in the simplest scenario for a system with pure three-wave mixing, implementations of this scheme are hindered by unwanted higher-order parametric processes that destabilize the system and add noise. We show analytically that detuning the two pumps from the sum and difference frequencies can stabilize the system and fully recover the BAE performance, enabling operation at otherwise inaccessible cooperativities. We also show that the acceleration demonstrated in a weak signal detection experiment [PRX QUANTUM 4, 020302 (2023)] was only achievable because of this detuning technique.

I. INTRODUCTION

Parametric processes such as amplification and frequency-conversion are crucial to the field of quantum information, with broad applications across quantum computing, quantum communication, and quantum sensing [1–7]. Processes that circumvent the quantum noise limit are of particular interest. A well-studied example uses two parametric pumps to evade the quantum backaction induced by measurement [8–12]. Unfortunately, these backaction-evading (BAE) schemes are often thwarted by higher-order nonlinearities. These nonlinearities yield undesired parametric processes which can add noise and cause unstable behavior in the system.

Across the various platforms that employ this style of measurement, several strategies have been developed to help mitigate these higher-order effects. Unfortunately, these strategies either add complexity or sacrifice other desirable features of the measurement. For microwave-frequency signals, three-wave mixing Josephson circuits can be designed to have a suppressed fourth-order (Kerr) nonlinearity [13, 14] at a single operating frequency [9] or over a range of frequencies with the addition of an extra flux bias [15]. For measurements of the state of a mechanical oscillator, a transient (pulsed) scheme has been demonstrated which intentionally induces mechanical instability [16]. Across both platforms, strategies that introduce destructive interference using additional pump tones have been proposed [17, 18] but these complicate the process of tuning to the correct operating point.

In this article, we present a simpler strategy to compensate the dominant fourth-order effects, unwanted single-mode squeezing (SMS), which diminish BAE performance and lead to instability. By introducing detunings to both of the parametric drives, we show that the BAE performance of the system can be completely recovered. Crucially, this technique does not require any additional control parameters such as flux biases or pumps that would add complexity, and it can be implemented at any bias point. Moreover, the technique can be readily combined with any of the aforementioned strategies to mitigate any residual SMS effects caused by imperfections in a Kerr-free device or by nonlinearities higher than fourth-order. We specifically discuss the technique in the context of one implementation of the two-tone BAE measurement: the gain and conversion (GC) microwave amplifier [10, 19, 20].

In Sec. II, we discuss the theoretical basis for the technique at the Hamiltonian level. In Sec. III, we characterize the technique for an open quantum system and we demonstrate analytically its effectiveness at recovering BAE performance. Finally, in Sec. IV, we describe how the technique can be applied to ultrasensitive quantum sensing experiments with a specific example from a recent BAE search for a microwave-frequency signal [10].

II. BACKACTION-EVADING HAMILTONIAN ENGINEERING

The model for the two-tone BAE system, as shown in Fig. 1(a), consists of a science mode A and a measurement mode B coupled with a state swapping interaction and a two-mode squeezing interaction with matched rates g. It is useful to consider an example for how this Hamiltonian may manifest in a physical system such that we can later discern how undesired SMS arises. To engineer this Hamiltonian between microwave-frequency modes using Josephson circuits, a three-wave mixing element (such as the Josephson ring modulator [3, 19, 21]) can be used to provide a trilinear term which mixes the superconducting phase φ across the science mode, the measurement mode, and a pump mode C such that it is of the form $\varphi_A\varphi_B\varphi_C$. When the C mode is driven strongly off its resonance, it can be treated as a classical pump field under the stiff pump approximation. The resulting interaction strength is then proportional to the amplitude of the pump field α. Driving the C mode at the sum and difference of the A and B mode frequencies

* These two authors contributed equally; direct correspondence to yue.jiang@jila.colorado.edu

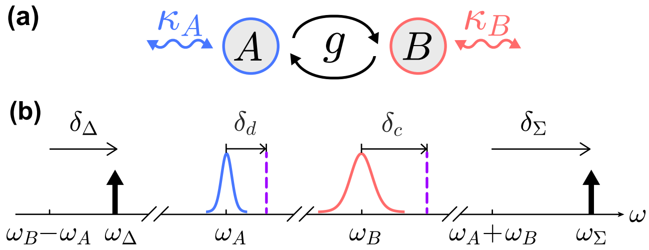

FIG. 1. (a) Simplified mode diagram of a BAE system. A science mode A (blue) and a measurement mode B (red) have external couplings κ_A and κ_B. The two modes are coupled by balanced two-mode squeezing and state-swapping interactions at a rate g. (b) Frequency diagram of the modes, pumps, reference frames, and detunings. The pump tones (black arrows) are detuned by δ_Δ and δ_Σ with respect to the difference and sum frequencies of the Kerr-shifted science and measurement mode frequencies ($\omega_{A,B}$). The Hamiltonian is written in the rotating frame of the half pump frequencies $(\omega_\Sigma \mp \omega_\Delta)/2$ for each mode (dashed purple lines).

($\omega_A+\omega_B$ and $\omega_B-\omega_A$) and matching the interaction rates results in the ideal balanced two-tone BAE Hamiltonian. Written in the rotating frame of the measurement mode ω_B, this Hamiltonian is given by

$$\hat{H}_{\mathrm{BAE}} = g\,(\hat{A}^\dagger \hat{B} + e^{-i\phi}\hat{A}^\dagger \hat{B}^\dagger) + \mathrm{h.c.} \quad (1)$$

where $\hbar = 1$, $\hat{A}$ and $\hat{B}$ are the annihilation operators for modes A and B, and ϕ is the relative phase between the two-mode squeezing and state-swapping drives. The phase ϕ determines the amplified quadrature, but will not change any of the results in the following discussion. Without loss of generality, we set ϕ to 0.

We can identify the BAE quadratures of interest by expressing the Hamiltonian in the quadrature basis. Defining the operator for a general quadrature as $\hat{X}_{M,\theta} = \frac{1}{\sqrt{2}}(e^{-i\theta}\hat{M} + e^{i\theta}\hat{M}^\dagger)$ for $M \in \{A, B\}$, we can express the BAE Hamiltonian in terms of $\hat{X}_M = \hat{X}_{M,0}$ and $\hat{Y}_M = \hat{X}_{M,\pi/2}$ as

$$\hat{H}_{\mathrm{BAE}} = 2g\hat{X}_A\hat{X}_B. \quad (2)$$

This Hamiltonian yields the Heisenberg equations of motion in the BAE quadratures of interest given by

$$d\hat{Y}_B/dt = -2g\hat{X}_A,\ d\hat{X}_A/dt = 0. \quad (3)$$

These equations indicate that the information contained in $\hat{X}_A$ appears at $\hat{Y}_B$ with noiseless amplification and that continuous measurement of $\hat{Y}_B$ does not perturb $\hat{X}_A$. Taken together, this implies that the measurement is BAE.

Unfortunately, higher-order nonlinearities intrinsic to the system Hamiltonian introduce additional parametric processes that diminish the BAE nature of the measurement. Of these, the leading-order effect is undesired single-mode squeezing (SMS). This SMS arises from four-wave mixing terms in the Hamiltonian of the form $\varphi_A^2\varphi_C^2$ and $\varphi_B^2\varphi_C^2$. We note that these four-wave-mixing terms additionally give rise to undesired frequency shifts in response to applied pump power, known as Kerr shifts. In this work, we assume that these Kerr shifts have already been accounted for, such that ω_A and ω_B describe the Kerr-shifted mode frequencies.

The specific choice of drive frequencies causes the four-wave-mixing terms to oscillate at $\omega_\Sigma + \omega_\Delta = 2\omega_B$ and $\omega_\Sigma - \omega_\Delta = 2\omega_A$. Written in the quadrature basis, this results in Hamiltonian terms that survive the rotating wave approximation (RWA) of the form

$$\hat{H}_{\mathrm{SMS}} = \frac{s_A}{2}\left(\hat{X}_A^2 - \hat{Y}_A^2\right) + \frac{s_B}{2}\left(\hat{X}_B^2 - \hat{Y}_B^2\right), \quad (4)$$

where s_A and s_B are the SMS rates for each mode. Given that they arise from terms that are quadratic in φ_C, s_A and s_B are both proportional to the pump power α^2, whereas the BAE interaction rate g is proportional to α. Including $\hat{H}_{\mathrm{SMS}}$ modifies the equations of motion, now given by

$$\begin{aligned} d\hat{Y}_B/dt &= -2g\hat{X}_A - s_B\hat{X}_B, \\ d\hat{X}_A/dt &= -s_A\hat{Y}_A, \\ d\hat{X}_B/dt &= -s_B\hat{Y}_B, \\ d\hat{Y}_A/dt &= -2g\hat{X}_B - s_A\hat{X}_A. \end{aligned} \quad (5)$$

From these modified equations, it is clear that the undesired SMS interactions degrade the BAE performance.

Fortunately, intentionally detuning the applied state swapping and two-mode squeezing drives from the difference and sum frequencies of the A and B modes can cancel the SMS effects on $\hat{X}_A$ and $\hat{Y}_B$. We define these intentional detunings δ_Σ and δ_Δ such that the applied pump frequencies are given by $\omega_\Sigma = \omega_A + \omega_B + \delta_\Sigma$ and $\omega_\Delta = \omega_B - \omega_A + \delta_\Delta$, as depicted by the horizontal arrows in Fig. 1(b).

To account for these detunings, the Hamiltonian should be expressed in the rotating frame defined by the modified pump frequencies as given by $(\omega_\Sigma - \omega_\Delta)/2 = \omega_A + \delta_d$ for the A mode and $(\omega_\Sigma + \omega_\Delta)/2 = \omega_B + \delta_c$ for the B mode. Here, $\delta_c = (\delta_\Sigma + \delta_\Delta)/2$ and $\delta_d = (\delta_\Sigma - \delta_\Delta)/2$ represent the common and differential detunings of the two pumps. The Hamiltonian (under the same RWA of Eqs. 2 and 4) can then be rewritten in this "half-pump" frame as $\hat{H} = \hat{H}_{\mathrm{BAE}} + \hat{H}_{\mathrm{SMS}} + \hat{H}_{\mathrm{DET}}$. $\hat{H}_{\mathrm{BAE}}$ and $\hat{H}_{\mathrm{SMS}}$ are unchanged in this new frame, but there are additional terms in the Hamiltonian resulting from the detunings. These additional terms take the form

$$\hat{H}_{\mathrm{DET}} = -\frac{\delta_d}{2}\left(\hat{X}_A^2 + \hat{Y}_A^2\right) - \frac{\delta_c}{2}\left(\hat{X}_B^2 + \hat{Y}_B^2\right). \quad (6)$$

In the quadrature basis, $\hat{H}_{\mathrm{DET}}$ looks very similar in form to $\hat{H}_{\mathrm{SMS}}$ as shown in Eq. 4.

We find that δ_d can be chosen to compensate the A mode squeezing on the BAE quadratures at $\delta_d = -s_A$, and that δ_c can be used to compensate the B mode

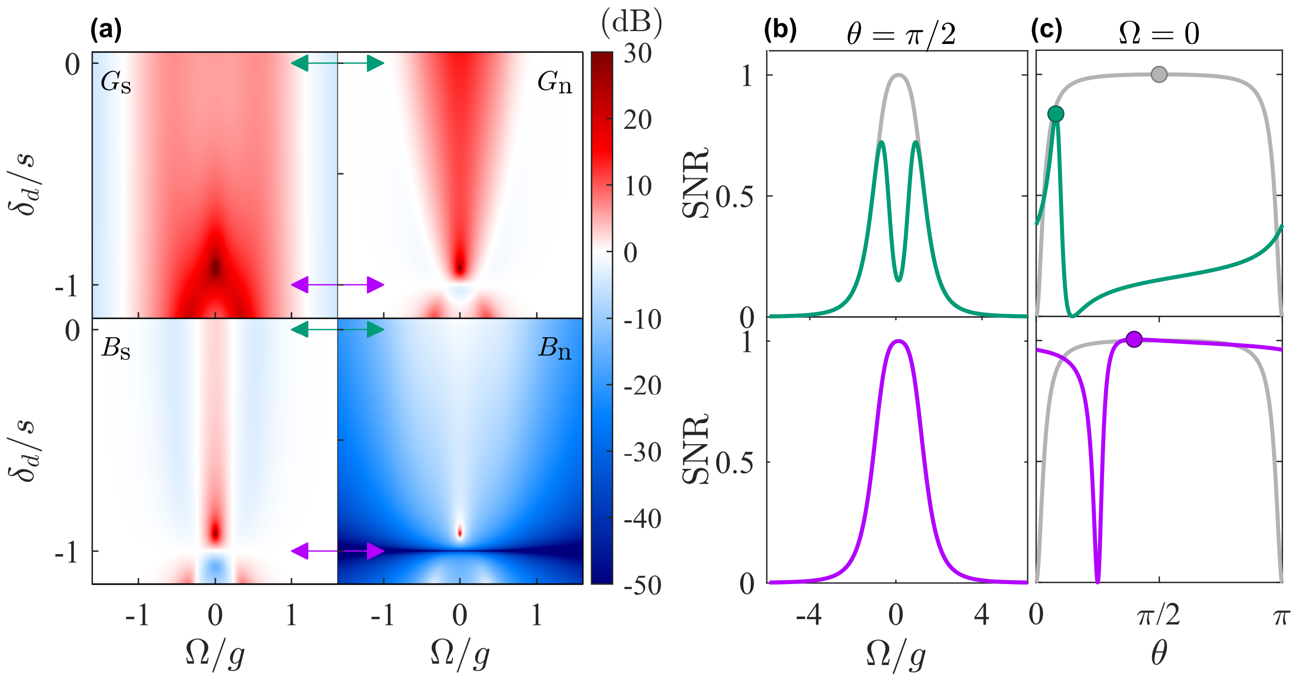

FIG. 2. SMS compensation with pump detunings. (a) Signal and noise gain as measured at $\hat{Y}_B$ (G_s and G_n) and backaction at $\hat{X}_A$ (B_s and B_n) for a sample set of conditions. We assume that $s_A = s_B = s$, $\kappa_A = \kappa_B = \kappa$, and $s = g/5 = \kappa/4$. The response when no compensatory detunings are applied ($\delta_d = \delta_c = 0$) is marked with a green double-headed arrow and the response when optimal detunings are applied ($\delta_d = -\delta_c = -s$) is marked with a purple arrow. (b) SNR(Ω) as measured at $\hat{Y}_B$, corresponding to a measurement angle of $\theta = \pi/2$. The SNR is normalized to the peak value of the $s = 0$ case (grey). With no detunings, the peak SNR is reduced due to reduced transmission gain and amplified measurement noise from squeezing. With optimal compensatory detunings, the SNR of the $s = 0$ case is completely recovered, indicating that BAE performance has been restored. (c) SNR(θ) for generalized quadratures as measured on resonance with the half-pump frame at $\Omega = 0$. With or without compensatory detunings, SMS shifts the optimal readout angle away from $\pi/2$ (away from $\hat{Y}_B$).

squeezing at $\delta_c = s_B$. With these compensatory detunings, the equations of motion become

$$\begin{aligned} d\hat{Y}_B/dt =& -2g\hat{X}_A, \\ d\hat{X}_A/dt =& 0, \\ d\hat{X}_B/dt =& -2s_B\hat{Y}_B, \\ d\hat{Y}_A/dt =& -2g\hat{X}_B - 2s_A\hat{X}_A, \end{aligned} \tag{7}$$

where the equations for the BAE quadratures of interest $\hat{X}_A$ and $\hat{Y}_B$ have been restored to their ideal forms given in Eq. (3). Operating at this point deposits all of the undesired effects induced by SMS into the unmeasured quadratures $\hat{X}_B$ and $\hat{Y}_A$.

The compensation technique works as long as the SMS and the BAE interactions arise from the same underlying nonlinearity. This is the case in Josephson circuits where both the third and fourth-order terms in the Hamiltonian arise from the Josephson nonlinearity. But in optomechanical systems, the origin of the parametric instability is less clear [11, 22], and in some cases may not be solved by pump detuning. In particular, the single-mode squeezing and instability observed in microwave frequency optomechanics is sometimes attributed to a parasitic thermal effect mediated by the mechanical oscillator's temperature-dependent resonance frequency [23]. Temperature oscillations are caused by the pump power oscillations at twice the mechanical frequency but they have a time delay. The delay causes the associated SMS Hamiltonian from Eq. 4 to have additional components of the form $\hat{X}_A\hat{Y}_A + \hat{Y}_A\hat{X}_A$ and $\hat{X}_B\hat{Y}_B + \hat{Y}_B\hat{X}_B$, precluding its compensation with pump detuning.

III. SQUEEZING COMPENSATION IN AN OPEN QUANTUM SYSTEM

To understand how squeezing compensation would manifest in the presence of noise and loss, we extend our analysis to study an open quantum system. We consider the A mode to be coupled to the signal at a rate κ_A, and the measurement mode to be coupled to the readout port at a rate κ_B, as shown in Fig. 1(a). We assume for simplicity that both modes have negligible internal loss, and that measurement noise enters at the B mode port. We derive the Heisenberg-Langevin equations from the full Hamiltonian with generalized detunings and squeezing rates. Solving the equations of motion in the frequency domain together with the input-output relations [24] yields the scattering parameters between the A and B ports. We express the scattering parameters in the quadrature basis as a function of Ω, the detuning from the half-pump frame. For example, we use $S_{Y_B X_A}$ to denote the output field at the $\hat{Y}$ quadrature of port B induced by the incoming field at the $\hat{X}$ quadrature of port A. These are given by

$$\begin{aligned} S_{Y_B X_A} =& 2g(i\Omega+\kappa_A/2)(i\Omega+\kappa_B/2)\sqrt{\kappa_A\kappa_B}/\beta, \\ S_{Y_B Y_A} =& -2g(s_A+\delta_d)(i\Omega+\kappa_B/2)\sqrt{\kappa_A\kappa_B}/\beta, \\ S_{Y_B X_B} =& \left(4g^2(s_A+\delta_d)+\beta_A(s_B-\delta_c)\right)\kappa_B/\beta, \\ S_{Y_B Y_B} =& 1-\beta_A(i\Omega+\kappa_B/2)\kappa_B/\beta, \end{aligned} \tag{8}$$

where the quantities

$$\begin{aligned} \beta_A &= (i\Omega+\kappa_A/2)^2-\left(s_A^2-\delta_d^2\right), \\ \beta_B &= (i\Omega+\kappa_B/2)^2-\left(s_B^2-\delta_c^2\right), \\ \beta &= \beta_A\beta_B-4g^2(s_A+\delta_d)(s_B+\delta_c), \end{aligned} \tag{9}$$

have been defined for simplicity.

We can directly see how compensation restores backaction evasion in the science quadrature of interest, $\hat{X}_A$, by studying another set of scattering parameters. These are given by

$$\begin{aligned} S_{X_A X_A} =& 1-\beta_B(i\Omega+\kappa_A/2)\kappa_A/\beta, \\ S_{X_A Y_A} =& \beta_B\left(s_A+\delta_d\right)\kappa_A/\beta, \\ S_{X_A X_B} =& -2g(s_A+\delta_d)(i\Omega+\kappa_B/2)\sqrt{\kappa_A\kappa_B}/\beta, \\ S_{X_A Y_B} =& 2g(s_A+\delta_d)(s_B+\delta_c)\sqrt{\kappa_A\kappa_B}/\beta. \end{aligned} \tag{10}$$

It is useful to group the first set of scattering parameters according to whether they describe the gain experienced by the signal or by the measurement noise. We therefore define the gain of the signal and noise as measured at $\hat{Y}_B$ as

$$\begin{aligned} G_{\rm s} &= |S_{Y_B X_A}|^2+|S_{Y_B Y_A}|^2, \\ G_{\rm n} &= |S_{Y_B X_B}|^2+|S_{Y_B Y_B}|^2. \end{aligned} \tag{11}$$

Similarly, the second set of scattering parameters describing backaction on $\hat{X}_A$ can be categorized according to

$$\begin{aligned} B_{\rm s} &= |S_{X_A X_A}|^2+|S_{X_A Y_A}|^2, \\ B_{\rm n} &= |S_{X_A X_B}|^2+|S_{X_A Y_B}|^2. \end{aligned} \tag{12}$$

In Fig. 2(a) we plot the set describing the signal and noise gain at $\hat{Y}_B$ and $\hat{X}_A$ ($\{G_{\rm s}, G_{\rm n}, B_{\rm s}, B_{\rm n}\}$) for a sample set of conditions. We assume for simplicity that the modes have equal external coupling rates κ and equal squeezing rates $s < \kappa, g$. Note that none of these assumptions are required for compensation.

Even when the squeezing rates are small compared to κ, when no compensatory detunings are applied (green double-headed arrow), the amplifier suffers both reduced signal transmission $G_{\rm s}$ and amplified measurement noise $G_{\rm n}$ as a result of the squeezing. The poor amplifier performance is a symptom of diminished backaction evasion. This assessment is confirmed by the non-zero transmission of noise B_n from the measurement port to $\hat{X}_A$, as can be seen in the bottom panel of Fig. 2(a). In contrast, when optimal compensatory detunings are applied (purple arrow), $B_n(\Omega) = 0$, indicating that BAE performance has been restored. It follows, therefore, that under these conditions, the measurement will not suffer amplified measurement noise at $\hat{Y}_B$.

From the signal and noise gain at $\hat{Y}_B$, the signal-to-noise ratio (SNR) is given as SNR $\propto G_{\rm s}/G_{\rm n}$. Figure 2(b) plots this SNR for the case of no compensatory detunings (green) and optimal detunings (purple), normalized to the ideal ($s = 0$) SNR (grey). When BAE performance is restored by optimal detunings, the ideal SNR is completely recovered when measuring $\hat{Y}_B$.

Crucially, detunings only recover BAE readout along $\hat{Y}_B$. The effects of the squeezing can still be seen when reading out other quadratures. Where before we considered measurements of $\hat{Y}_B$ ($\theta = \pi/2$), in Fig. 2(c) we instead measure along a generalized quadrature parameterized by θ and plot the SNR at the half-pump frequency ($\Omega = 0$). Uncompensated SMS (green line) causes a reduced SNR in almost all quadratures relative to the $s = 0$ case (grey), and we see that reading out at $\theta = \pi/2$ is no longer optimal in this case. Instead, the SNR is maximized along the quadrature marked by the green point that experiences squeezed measurement noise rather than amplified signal. Because the signal is not amplified along this quadrature, the SNR is highly sensitive to deviations in θ as compared to the more flat-topped $s = 0$ case.

In comparison, when compensatory detunings are applied (purple line), we see that the optimal readout quadrature is largely insensitive to small changes in θ due to the recovered signal amplification. Additionally, there is actually a modest increase to the peak SNR as compared to the $s = 0$ case. This improvement comes from sacrificing some signal amplification in exchange for squeezed measurement noise along a quadrature marked by the purple dot. In fact, if it were possible to measure along a different quadrature at each frequency Ω, the inadvertent squeezing effects could be leveraged to enhance the SNR over the whole measurement range. This could potentially be implemented by applying a frequency-dependent phase shift to the fields exiting the measurement port such that the readout angle is optimized separately for each Fourier component [25].

One should note that detuning compensation restores the BAE performance in quadratures defined in the half-pump frame rather than in the mode frame. The measurement's sensitivity will therefore peak for forces driving the A mode at the half-pump frequency $\omega_A + \delta_d$ marked by the purple dashed line in Fig. 1(b) instead of at ω_A. Fortunately, because the peak sensitivity is fully recovered, as long as the experimentalist is aware of this shift, it can easily be accounted for in experiment.

Beyond just destroying the BAE performance, unde-

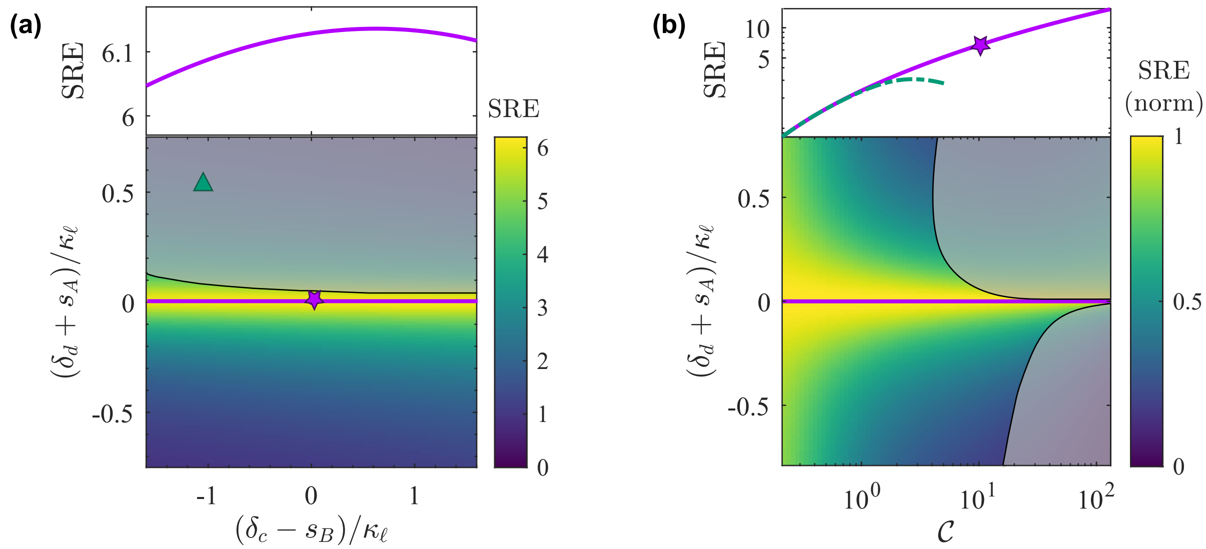

FIG. 3. Scan rate enhancement in the GC-enhanced search for a weak microwave signal at unknown frequency in the presence of unwanted SMS. (a) SRE as a function of pump detunings which are varied about their optimal values ($-s_A$ and s_B). Operating points with zero and optimal detunings are marked by the green triangle and purple star. The grey shaded region marks the unstable regime. The condition for canceling the SMS of the science mode satisfies $\delta_d = -s_A$ and is marked by a purple line. The SRE along this line is plotted in the top panel. (b) Robustness of compensation procedure to increased cooperativity $\mathcal{C}$. Upper panel: SRE increases with cooperativity, but uncompensated SMS causes the SRE to turn over (green dashed line) due to amplified measurement noise. The squeezing additionally causes the system to become unstable where the green dashed line ends. Detuning compensation protects the system from these effects, enabling a six-fold acceleration to be achieved and preserving stability as the cooperativity is increased (purple line). Bottom panel: SRE normalized to its optimally compensated value at a given cooperativity. With increased cooperativity, the narrowing of the yellow band reveals an increase in sensitivity to the detuning control parameters. The unstable regime approaches the line of compensation asymptoptically with increased cooperativity (bottom panel), making further SRE beyond $\mathcal{C} = 10.4$ (purple star) difficult to achieve.

sired SMS causes these measurement schemes to become unstable, placing a hard limit on the achievable cooperativity. The poles of the scattering parameters (the roots of β) give the criteria for stability. The existence of a root with a negative imaginary component signifies that the system is unstable. While squeezing destabilizes the system, compensatory detunings counteract the destabilization such that the point of optimal compensation $\delta_d = -s_A$ and $\delta_c = s_B$ is always stable for any combination of the squeezing rates.

IV. IMPLEMENTATION FOR QUANTUM SENSING

In Sec. III, we made the simplifying assumptions that internal loss was negligible compared to the external coupling rates ($\kappa_\ell \ll \kappa_A, \kappa_B$), and that the coupling rates were equal ($\kappa_A = \kappa_B$). While these assumptions generally hold true for amplifiers used in quantum signal processing applications [21], this is not usually the case for ultrasensitive quantum sensing applications where the signal is weakly coupled to the science mode [11, 26]. In this section, we extend our analysis to consider this quantum sensing application. We treat the system under the assumptions that the internal loss κ_ℓ of the science mode dominates over its weak coupling to the signal κ_A, and that both of these rates are small compared to the measurement port coupling rate ($\kappa_A \ll \kappa_\ell \ll \kappa_B$). We maintain the assumption that the internal loss of the measurement mode is negligible.

In order to focus discussion, we consider one particular sensing application: the search for a weak microwave signal at an unknown frequency, a problem of particular interest for axion dark matter searches [26]. Recently, the two-tone BAE measurement technique was applied to an experiment designed to mimic a real axion search, and a six-fold acceleration to the spectral scan rate was demonstrated [10]. This acceleration was only possible by successfully canceling undesired SMS using the compensatory detuning scheme described in this paper.

In this section, we analytically predict the scan rate enhancement (SRE) using the system parameters from the axion search demonstration experiment [10]. We take $g/2\pi = 7.3$ MHz, $\kappa_\ell/2\pi = 960$ kHz, and $\kappa_B/2\pi = 20.6$ MHz. The squeezing rates s_A and s_B are estimated to be around 7% and 14% of the GC interaction rates g respectively. Following the procedure outlined in Sec. III, we calculate the scattering parameters and the SNR for this system. The spectral scan rate scales as $\int (\mathrm{SNR})^2 d\Omega$. The SRE can then be calculated by comparing the scan rate to that of a quantum-limited search. A more detailed discussion of this calculation can be found in Ref. [10].

The SRE for various combinations of pump detunings is given in Fig. 3(a), where the unstable regime is represented by the grey shaded area. Because $s_B \ll \kappa_B$ for this system, the squeezing of the B mode has a negligible effect on the system, and it is mainly the A mode squeezing that matters for performance and stability. When no pump detunings are applied ($\delta_c = \delta_d = 0$), the system is already unstable. At the optimal cancellation point, ideal ($s = 0$) amplifier performance is recovered and the system is stabilized.

Further SRE can theoretically be achieved by pumping harder, corresponding with increased interaction rates g and cooperativity $\mathcal{C} = \frac{4g^2}{\kappa_B(\kappa_\ell + \kappa_A)}$. However, because $g \propto \alpha$ while $s_A, s_B \propto \alpha^2$, pumping harder also increases the squeezing rates relative to both g and the damping rates. It is therefore important to consider the robustness of the compensation to increased cooperativity.

In Fig. 3(b), the interaction rate g and the squeezing rates s_A and s_B are increased according to their dependence on the pump strength α. In the upper panel, we plot the SRE for optimal detunings (purple, $\delta_c = -s_A, \delta_d = s_B$) and zero detunings (green, $\delta_c = \delta_d = 0$). The zero detunings line ends when the system would become unstable. In this case, the maximum SRE that could have been achieved was SRE $= 3.1$ and the system would have become unstable at cooperativity $\mathcal{C} = 5.3$. With detunings, $\mathcal{C} = 10.4$ was achieved, resulting in a scan rate enhancement of SRE $= 5.6$ [10]. We suspect that the measured SRE is smaller than we predict analytically because the experimental operating point was not exactly the optimal compensatory point. The sensitivity of the mode frequencies to fluctuations in the magnetic flux threading the Josephson ring modulator led to challenges identifying and remaining at the desired operating point, as discussed in [10].

While the compensation is robust (and the system stable) to arbitrarily high cooperativity, the experimental bound on tuning accuracy ultimately limits this quantity. In the bottom panel of Fig. 3(b), δ_c is chosen to be optimal ($\delta_c = s_B$) while δ_d is varied about its optimal value. We see that when s_A becomes large enough that the system would be unstable in the absence of detunings (which occurs at $\mathcal{C} = 5.3$), the instability begins to approach the line of perfect cancellation asymptotically. In the demonstration experiment, the cooperativity was limited to $\mathcal{C} = 10.4$ for this reason. Experimentally, increasing the interaction rates beyond this point while maintaining the desired amplifier performance became more challenging.

V. CONCLUSION AND OUTLOOK

The detuning-based technique presented in this article provides a simple strategy for compensating the effects of undesired SMS in two-tone BAE measurements. The compensation scheme could benefit systems both with and without intentional Kerr-suppression while adding very little complexity. This ultimately allows for BAE operation at cooperativities beyond the threshold where destabilizing effects from SMS would have otherwise ruined performance.

While compensatory detunings theoretically allow for operation at arbitrarily high cooperativity without inducing instability or amplified noise, the unstable regime asymptotically approaches the compensatory operating point. The limiting factor on these detuned BAE schemes then becomes the sensitivity of the system to frequency drifts of the pump tones or modes. Technical improvements in these areas could allow for operation at higher cooperativities than have been achieved thus far.

The detuning compensation solution also introduces opportunities to improve on the traditional BAE scheme by further increasing the SNR. By measuring along a slightly different quadrature from the one that is amplified, experiments could leverage the effects of the undesired SMS to achieve both signal amplification and squeezed measurement noise. By applying a frequency-dependent phase shift to the fields exiting the measurement port, the SNR would be enhanced over the entire measurement range as compared to the case with no squeezing.

ACKNOWLEDGEMENTS

The authors thank John Teufel for useful discussions regarding potential applications of this work to the field of optomechanics. This document was prepared with support from the resources of the Fermi National Accelerator Laboratory (Fermilab), the U.S. Department of Energy, the Office of Science, and the HEP User Facility. Fermilab is managed by Fermi Research Alliance, LLC (FRA), acting under Contract No. DE-AC02-07CH11359 and the NSF award 2209522. Additionally, this work was supported by Q-SEnSE: Quantum Systems through Entangled Science and Engineering (NSF QLCI Award OMA-2016244) and the NSF Physics Frontier Center at JILA (Grant No. PHY-1734006).

[1] Warwick P Bowen, Nicolas Treps, Ben C Buchler, Roman Schnabel, Timothy C Ralph, Hans-A Bachor, Thomas Symul, and Ping Koy Lam. Experimental investigation of continuous-variable quantum teleportation. *Physical Review A*, 67(3):032302, 2003.

[2] Samuel L Braunstein and Peter Van Loock. Quantum information with continuous variables. *Reviews of modern physics*, 77(2):513, 2005.

[3] N. Bergeal, R. Vijay, V. E. Manucharyan, I. Siddiqi, R. J. Schoelkopf, S. M. Girvin, and M. H. Devoret. Analog information processing at the quantum limit with a Josephson ring modulator. *Nature Physics*, 6(4):296–302, 2010.

[4] R. Vijay, D. H. Slichter, and I. Siddiqi. Observation of quantum jumps in a superconducting artificial atom. *Physical Review Letters*, 106(11):110502, 2011.

[5] Schwab Gigan, HR Böhm, Mauro Paternostro, Florian Blaser, G Langer, JB Hertzberg, Keith C Schwab, Dieter Bäuerle, Markus Aspelmeyer, and Anton Zeilinger. Self-cooling of a micromirror by radiation pressure. *Nature*, 444(7115):67–70, 2006.

[6] Markus Aspelmeyer, Tobias J Kippenberg, and Florian Marquardt. Cavity optomechanics. *Reviews of Modern Physics*, 86(4):1391, 2014.

[7] K. M. Backes, D. A. Palken, S. Al Kenany, B. M. Brubaker, S. B. Cahn, A. Droster, Gene C. Hilton, Sumita Ghosh, H. Jackson, S. K. Lamoreaux, et al. A quantum enhanced search for dark matter axions. *Nature*, 590(7845):238–242, 2021.

[8] Anja Metelmann and Aashish A Clerk. Nonreciprocal photon transmission and amplification via reservoir engineering. *Physical Review X*, 5(2):021025, 2015.

[9] T.-C. Chien, O. Lanes, C. Liu, X. Cao, P. Lu, S. Motz, G. Liu, D. Pekker, and M. Hatridge. Multiparametric amplification and qubit measurement with a kerr-free Josephson ring modulator. *Physical Review A*, 101(4):042336, 2020.

[10] Y Jiang, EP Ruddy, KO Quinlan, M Malnou, NE Frattini, and KW Lehnert. Accelerated weak signal search using mode entanglement and state swapping. *PRX Quantum*, 4(2):020302, 2023.

[11] JB Hertzberg, T Rocheleau, T Ndukum, M Savva, Aashish A Clerk, and KC Schwab. Back-action-evading measurements of nanomechanical motion. *Nature Physics*, 6(3):213–217, 2010.

[12] J Suh, AJ Weinstein, and KC Schwab. Optomechanical effects of two-level systems in a back-action evading measurement of micro-mechanical motion. *Applied Physics Letters*, 103(5):052604, 2013.

[13] N. E. Frattini, U. Vool, S. Shankar, A. Narla, K. M. Sliwa, and M. H. Devoret. 3-wave mixing Josephson dipole element. *Applied Physics Letters*, 110(22):222603, 2017.

[14] V. V. Sivak, N. E. Frattini, V. R. Joshi, A. Lingenfelter, S. Shankar, and M. H. Devoret. Kerr-free three-wave mixing in superconducting quantum circuits. *Physical Review Applied*, 11(5):054060, 2019.

[15] A. Miano, G. Liu, V. V. Sivak, N. E. Frattini, V. R. Joshi, W. Dai, L. Frunzio, and M. H. Devoret. Frequency-tunable kerr-free three-wave mixing with a gradiometric snail. *Applied Physics Letters*, 120(18):184002, 2022.

[16] Robert D Delaney, Adam P Reed, Reed W Andrews, and Konrad W Lehnert. Measurement of motion beyond the quantum limit by transient amplification. *Physical review letters*, 123(18):183603, 2019.

[17] Steven K Steinke, KC Schwab, and Pierre Meystre. Optomechanical backaction-evading measurement without parametric instability. *Physical Review A*, 88(2):023838, 2013.

[18] K Wurtz, BM Brubaker, Y Jiang, EP Ruddy, DA Palken, and KW Lehnert. Cavity entanglement and state swapping to accelerate the search for axion dark matter. *PRX Quantum*, 2(4):040350, 2021.

[19] Baleegh Abdo, Archana Kamal, and Michel Devoret. Nondegenerate three-wave mixing with the Josephson ring modulator. *Physical Review B*, 87(1):014508, 2013.

[20] A. Roy and M. Devoret. Introduction to parametric amplification of quantum signals with Josephson circuits. *Comptes Rendus Physique*, 17(7):740–755, 2016.

[21] N. Bergeal, F. Schackert, M. Metcalfe, R. Vijay, V. E. Manucharyan, L. Frunzio, D. E. Prober, R. J. Schoelkopf, S. M. Girvin, and M. H. Devoret. Phase-preserving amplification near the quantum limit with a Josephson ring modulator. *Nature*, 465(7294):64–68, 2010.

[22] Itay Shomroni, Amir Youssefi, Nick Sauerwein, Liu Qiu, Paul Seidler, Daniel Malz, Andreas Nunnenkamp, and Tobias J Kippenberg. Two-tone optomechanical instability and its fundamental implications for backaction-evading measurements. *Physical Review X*, 9(4):041022, 2019.

[23] Junho Suh, MD Shaw, HG LeDuc, AJ Weinstein, and KC Schwab. Thermally induced parametric instability in a back-action evading measurement of a micromechanical quadrature near the zero-point level. *Nano letters*, 12(12):6260–6265, 2012.

[24] D.F. Walls and G.J. Milburn. *Quantum Optics*. Springer Berlin Heidelberg, 2008.

[25] L McCuller, C Whittle, D Ganapathy, K Komori, M Tse, A Fernandez-Galiana, L Barsotti, Peter Fritschel, M MacInnis, F Matichard, et al. Frequency-dependent squeezing for advanced ligo. *Physical review letters*, 124(17):171102, 2020.

[26] P. Sikivie. Detection rates for "invisible"-axion searches. *Physical Review D*, 32:2988–2991, 1985.